© 2017 IJSRSET | Volume 3 | Issue 5 | Print ISSN: 2395-1990 | Online ISSN : 2394-4099
Themed Section: Engineering and Technology

CFD Analysis of Flow Metering of Non-Newtonian Fluids by Rotameter

Chandan Raju B C*[1], Yogesh Kumar K J[2], Dr. V Seshadri[3]
*[1]M. Tech. Student, Thermal Power Engineering, MIT-Mysore, Karnataka, India
[2]Assistant Professor, Department of Mechanical Engineering, MIT-Mysore, Karnataka, India
[3]Professor (Emeritus), Department of Mechanical Engineering, MIT-Mysore, Karnataka, India

ABSTRACT

Rotameter is a variable area type of flow meter that can be used to measure the flow rates of both liquid and gases. Normally the rotameters are calibrated either with water or air depending on their applications. However, when the rotameter is used for other fluids, correction factors need to be applied for variations in fluid density and viscosity. These factors are not very well established. In the present work, CFD has been used to analyse characteristics of rotameter with non-standard fluids. A CFD methodology has been developed using ANSYS software-15 and it is validated using the available data. The most suitable choice of turbulence model is identified. The semi divergence angle (θ) of the rotameter plays on important role in deciding the range of flow rates for a given meter. CFD has been used quantify the range of flow rates for various values of θ in the range 0.5 to 2°. The relation is found to be non-linear. The characteristics of a rotameter used for measuring non-Newtonian fluids are also analysed. The drag characteristics of a viscosity compensating float inside a tube for the flow of pseudo plastic fluid are studied for various values of k and n. Such analyses are made at two diameter ratios and two Reynolds numbers in the laminar regime. It is observed that C_D is affected by the value of n. The performance of a rotameter with pseudo plastic fluid having different values of consistency index (k) and power law index (n) are analysed and they are compared with water performance. It is observed that the indicated flow in case of non-Newtonian fluid will always less than actual flow. The maximum error will be of the order of 5% as long as care is taken to ensure that the range of Reynolds numbers in both water as well as non-Newtonian fluid flow are kept same. This conclusion is valid for flow rates in the laminar regime only.

Keywords: CFD, ANSYS, ISO, RANS, SST, FDM, FEM, ANSYS FLUENT

I. INTRODUCTION

Flow meter is a device that measures the flow rate of any liquid in an open or closed conduit. Flow meters that are used in the industry for different applications. Some of the widely used types of flow meters are follows.

- **Differential pressure flow meters:** Flow meters like orifice meter, Flow nozzles and venturi meter etc.
- **Velocity flow meters:** Flow meters like turbine flow meter, Vortex flow meter, Electromagnetic flow meter, Ultrasonic Doppler flow meter etc.
- **Mass flow rate:** Flow meters are under this category are Thermal flow meters, Corioils flow meter etc.
- **Special flow meters:** turbine flow meter, positive displacement meters, V cone flow meter etc.

Rotameter is a variable area type of flow meter .It consists of a vertically placed glass tapered tube and metallic float within the tube which is free to move up and down. The metering tube placed vertically along with fluid stream with a larger diameter at the top. Fluid enters at the bottom of the tube and passes over the float and leaves at the top.

The maximum diameter of float is approximately same as the bore of the tube. When fluid enters at the bottom of tube float start rises in the tube. When there is no flow through the meter, the float is at the bottom of the metering tube. When fluid enters the metering tube, the buoyant effect and drag force effect will act on the float but float density higher than the liquid, position of float still in the bottom of tube. With upward movement of float towards

the larger end of the tapered tube. When buoyant force and drag force of the fluid on the float is same as that of weight of float, then the float is in dynamic equilibrium. If there is an increase in the flow rate. It causes the float to rise higher in the tube where as a decreasing the flow rate causes drop in height of the float in the tube. Every float position corresponds to a particular flow rate of the fluid. So flow rate can be measured in the rotameter by observation of the position of float in the metering tube.

Principle of Rotameter

Consider a rotameter and various forces that are acting on the float at any given position are as shown in Fig.1 they are also follows.

1. The weight of the float (W) which is acting on vertically downwards.
2. The buoyant force (F_B) acting on vertically upwards.
3. The drag force (F_D) due to fluid flow acting on vertically upwards.

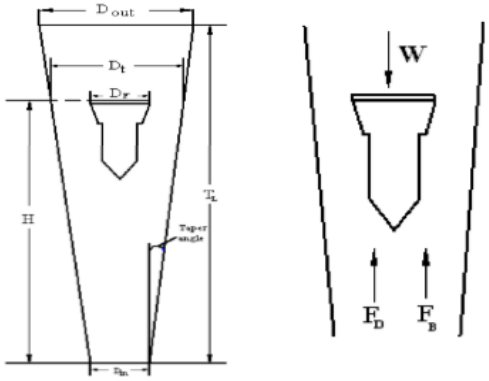

Figure 1. Geometry of Rotameter and Various Forces acting on the Float

The above Fig. shows the rotameter with float inside the tapered tube and the various forces acting on the float. In the above first two forces namely weight of float (W) and buoyant force (F_B) are constant for a given meter. However, the drag force (F_D) is dependent on various factors such as, the shape of float, velocity of fluid, diameter ratio of the float to the tube etc.

When the all forces are in equilibrium position then Equation becomes

$$F_D = W - F_B \quad \ldots\ldots (1)$$

Where

F_D= Drag force of the fluid

F_B = Buoyant force

W= Weight of the float

Weight of the float acting downward due to gravity (W) is given by:

$$W = V_F.\rho_S.g \quad \ldots\ldots (2)$$

Where

ρ_S= density of float

V_F= volume of float

g =gravitational force

Buoyant force of fluid acting on the float is given by

$$F_B = V_F.\rho_F.g \quad \ldots\ldots (3)$$

Where

ρ_F=density of fluid

Drag force of the fluid acting on the float is given by

$$F_D = 0.5 * C_D.\rho_F.U_{ann}{}^2.A_S \quad \ldots\ldots (4)$$

Substitute Equation (3) and (4) in Equation (1) we get

$$F_D = W - F_B = (\rho_S - \rho_F)\, g.V_F$$

$$= 0.5 * C_D.\rho_F.U_{ann}{}^2.A_S \quad \ldots\ldots (5)$$

The flow rate is given by the continuity Equation:

$$Q = (U_{in} \times A_{in}) = (U_{anu} \times A_{anu})$$

$$= \frac{\pi}{4}(D_t^2 - D_F^2) \times U_{anu} \quad m^3/s \quad \ldots\ldots (6)$$

Where

D_t =Diameter of the tube when float is in equillibrium position.

D_F= Maximum Diameter of the float.

A_{in}= Inlet c/s area of the tube.

Uann= Average velocity in the annular area between the float and the tube

A_{anu}= Annulus Area between the float and tube.

From the Equation (4) U_{anu} can also be written as

$$U_{anu} = \sqrt{\frac{2(\rho_S - \rho_F)\, g.V_F}{C_D.\rho_F.A_S}} \quad m3/s \quad \ldots\ldots (7)$$

Substitute Equation (6) in Equation (7) we get

$$Q = \frac{\pi}{4} \times (D_t^2 - D_F^2) \times \sqrt{\frac{2(\rho_S - \rho_F)\, g.V_F}{C_D.\rho_F.A_S}} \quad m^3/s \quad \ldots\ldots (8)$$

The half divergence angle of the tapered tube is given by

$$\tan\boldsymbol{\theta} = \frac{D_{out} - D_{in}}{2TL} \quad \ldots\ldots (9)$$

Where

D_{in} =inlet diameter of tube

D_{out}= outlet diameter of tube

T_L = vertical height of tube

Consider the equation for the tapered tube from the relation

$D_T = D_F + 2\ H \tan\theta$

$(D_t^2 - D_F^2) = 4.H.D_s.\tan\theta + 4.H^2.(\tan\theta)^2$ ……..……..(10)

Substitute Equation (8) in Equation (10) we get

$$Q = \frac{\pi}{4}[4.H.D_F.\tan\theta + 4.H^2.(\tan\theta)^2] \times \sqrt{\frac{2(\rho_S - \rho_F)\ g.V_F}{C_D.\rho_F.A_S}} \quad m^3/s \ \ldots.. (11)$$

The above Equation gives the relation between the flow rates of fluid, position of float of any given Rotameter.

Density Correction Factor

A rotameter can be used to measure the liquid flow rate having different viscosity and density. The changes in the density of fluid will affect flow rate of measured value significantly, but changes in viscosity of fluid will not have a major effect of flow rate. This is due to the fact that C_D is not very sensitive Reynolds number in the turbulent resume. Density correction factor to measure the flow rate of different fluid can be derived as follows.

Volumetric flow rate of water in the rotameter is given by

$$Q_w = \frac{\pi}{4}[4.H.D_F.\tan\theta + 4.H^2.(\tan\theta)^2] \times \sqrt{\frac{2(\rho_S - \rho_w)\ g.V_F}{C_D.\rho_F.A_S}} \quad m^3/s \ \ldots. (12)$$

Where

Q_W= volumetric flow rate of water

ρ_w= density of water

H= Height

Suppose same Rotameter is used to measure flow rate of fluid, then adjusted flow rate until float reaches the same height of h

$$Q_L = \frac{\pi}{4}[4.H.D_F.\tan\theta + 4.H^2.(\tan\theta)^2] \times \sqrt{\frac{2(\rho_S - \rho_L)\ g.V_F}{C_D.\rho_F.A_S}} \quad m^3/s \ \ldots. (13)$$

Where

ρ_L= density of any liquid

Dividing Equation (13) and (12)

$$Q_L = \sqrt{\frac{(\rho_S - \rho_L)\rho_w}{(\rho_S - \rho_w)\rho_L}} * Q_W \quad m^3/s \ \ldots (14)$$

There fore

$$Q_L = C_S.Q_W \quad \ldots\ldots\ldots\ldots\ldots (15)$$

Where

C_S= density correction factor

$$C_S = \sqrt{\frac{(\rho_S - \rho_L)\rho_w}{(\rho_S - \rho_w)\rho_L}} \quad \ldots\ldots\ldots\ldots\ldots\ldots (16)$$

II. LITERATURE REVIEW

A. Review of the Previous Work

Several investigators have used CFD to analysis the flow through different life's of flow meters under varying both standard and non-standard conditions.

Arun et.al [1] has used to analyse flow through a Venturimeter which is a typical type pressure based flow meter that is widely used in the industries applications. The ISO 5167 standards provide the value of C_d for the Venturimeter with an order of Reynolds number (Re) above $2x10^5$ In some cases of viscous fluid, Venturimeters are sometimes operated in laminar flow regime and also in turbulent regime at Re below the range specified in the standard. In this work analysis is made to study and prepare a computational model of Venturimeter, but which can be used for efficient and also easy means for predicting the C_d at low Reynolds numbers (Re). CFD software ANSYS fluent14.0 has been used as a tool for perform the modelling and simulation of the Venturimeter. Simulation is carried by standard Venturimeter and then the results were validated with results specified in the standards. The results of the simulations show that the C_d decreases rapidly as the Re decreases. Then the results were compared with the analytically proposed equation to calculate the value of C_d at low Reynolds number.

Rakesh Joshi et.al [2] studied the effect of rotameter float design on the performance characteristics of rotameter. They concluded that small changes in flow rate cannot be detected by rotameter under normal operating conditions. The geometry of the float needs to be designed carefully in order to increase the sensibility.

Prasanna et.al [**3**] conducted CFD analyses on compressibility effects of orifice plate and venturimeter and type of flow meters. They have chosen both concentric standard orifice plate as well as quarter circle orifice plate. The computed values of discharge co efficient, expansibility factor and permanent pressure loss coefficient are agrees with the standards values over a wide range of Reynolds number, diameter ratio.

Deepu et.al [4] conducted experiments in CFD tool ANSYS Fluent 14 software to study the design of Rotameter using CFD. In the design of rotameter, coefficient of drag (C_D) of the float is a very important parameter. They have derived a correlation for C_D as a function of diameter ratio. Further, they concluded that any disturbance up stream should be at a distance of

more than 5D from the entrance of the rotameter in order to ensure that the accuracy of rotameter is not affected significantly.

Pavan Kumar et.al [5] conducted experiments in CFD tool using ANSYS FLUENT 14 software to study the analysis of flow through a Rotameter that was available in fluid mechanics laboratory of their Institute. Here the geometry was considered as the 2D axisymmetric and meshing of geometry done by axisymmetric quadrilateral elements. Water is considered as fluid and steel is used as the float .From the experiments it is concluded that use of CFD gives good accuracy results within ± 1 % error and the drag force will remain same over the entire range of flow rates. They also have studied the effect of change in the density and viscosity of the fluid on the performance of rotameter.

B. Scope of Present Work

Based on the review of previous work done the following scope of the work is finalized.

- Development of validated CFD methodology to analyse the flow through rota meters. The validation will be done using data on existing rotameter.
- The angle of divergence of the tapered tube is one of the major parameters which affects the range of flow rates that can be measured by a given rotameter having specified height. Hence in order to quantify this effect it is proposed to systematically vary angle of divergence and analyse its effect on the maximum flow rate that can be measured.
- The analysis of flow of non-Newtonian fluid through a rotameter will be investigated. As a first step the effect of non-Newtonian behaviour of the fluid on the drag force of viscosity compensating float inside a tube is analysed. The non-Newtonian fluid is modelled as a pseudo plastic (power law fluid). Analysis are to be made for various values of power law consistency index (k) and power law index (n).

The flow of pseudo plastic fluid through on actual rotameter will be analysed the various values of k and the results will be compared with water data and deviations in the meter reading will be quantified.

III. CFD METHODOLOGY ANDVALIDATION

A. CFD Methodology

CFD methodology for analysing the flow through the rotameter assumes fluid to be Newtonian fluid and flow to be axisymmetric. The governing equations used to solve this problem are continuity equation, momentum equations with proper boundary conditions. However, if the flow is turbulent, Reynolds averaged momentum equations (RANS) are to be solved and additional equations are used with appropriate boundary conditions. Hence if the flow is turbulent, different turbulence models are used in this analysis like k- omega- SST standard- k-epsilon and standard-k-omega. CFD software uses numerical techniques like finite difference method (FDM), finite volume method (FVM), and finite element method (FEM) to solve the equations and arrives at the solution in an iterative manner.

In the present study ANSYS FLUENT – 15 software, with 2D axisymmetric with proper boundary conditions and mesh convergence is used to get required solution.

B. Validation of CFD Methodology

Analysis of Flow through an Actual Rotameter

Pavan Kumar et.al [5] has analysed the flow of water through a rotameter existing in fluid mechanics laboratory of the Institute. The range of rotameter was 0-40 lpm and the various dimensions are given in Table 3.5.

Variables	Values	Units
Inlet diameter(D_{in})	25.48	mm
Outlet diameter (D_{out})	36.85	mm
Tube height(H)	260	mm
Half tapered angle($\boldsymbol{\theta}$)	1.12°	Degree

Table: 3.5 Boundary Conditions Used for the Analysis of Rotameter

Dimensions of the Tapered Tube:

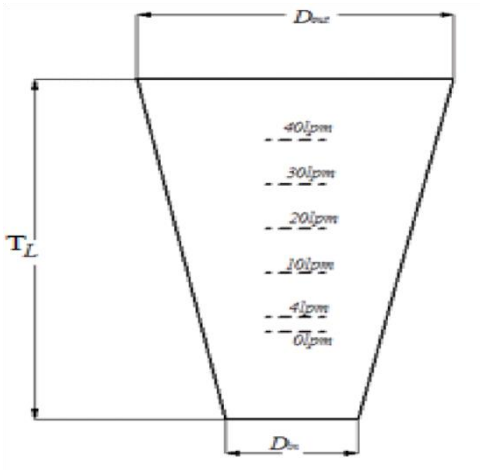

Fig.3.4 Dimensions of Tapered Tube

Dimensions of the float:

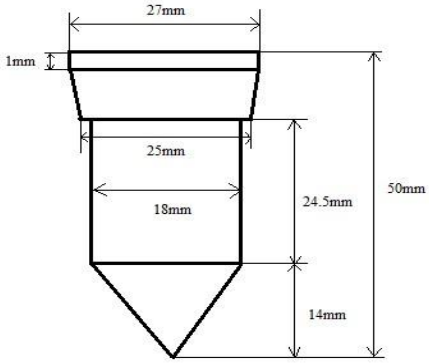

Fig.3.5 Dimensions of the Float

Dimensions of the Floa

Float Material = stainless steel

Material Density = ρ_F= 7850 kg/m^3

Volume of float= V_F = 12584.46 mm^3

Equilibrium Drag force F_D is calculated using the formula.

$F_D = [(\rho_F - \rho_W) \times V_F \times g] = (7850 - 1000) \times 12584.46 \times 10^{-9} \times 9.81 = 0.8456$ N

The dimensions of the float and the geometry of the rotameter are given in Figs.3.5. And 3.6The flow through this rotameter is analysed for various positions of the float in order to verify the accuracy of the meshing and validity of the computations. At any given position of the float. The inlet velocity corresponding to the flow rate marked at that position is specified. The drag force on the float is calculated from this CFD analysis and ideally this should be equal to 0.8456 N which will ensure equilibrium of the float at that position. Such analyses have been made for 8 positions given in the Table.3.6.

Q_{ind} (lpm)	H (mm)	$\frac{D_F}{D_t}$
4	57.5	0.96
7	72.5	0.94
10	86.5	0.92
15	108.5	0.89
20	129	0.87
25	148	0.84
30	166	0.82
35	183	0.81
40	199	0.79

Table 3.6: Height of markings from Inlet (Float Height)for different Flow Rates and Diameter Ratio at that Position

Modelling

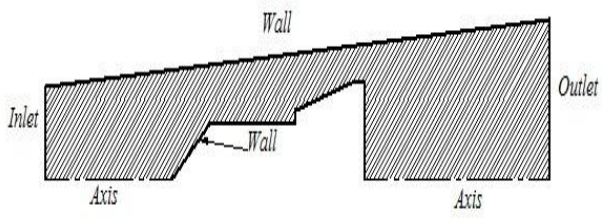

Fig 3.6: Geometry and Boundary Conditions Used for the Analysis of Actual Rotameter

The above Fig.3.6 shows the geometry of flow domain and boundary conditions used in CFD analysis. The geometry considered as 2D symmetric and hence only half of the domain is modelled. Flow rate markings are in the range of 4-40 lpm and the different heights of each marking from the inlet and diameter of tapered tube and diameter ratio of the float at different heights are tabulated in the above Table 3.6.

Meshing

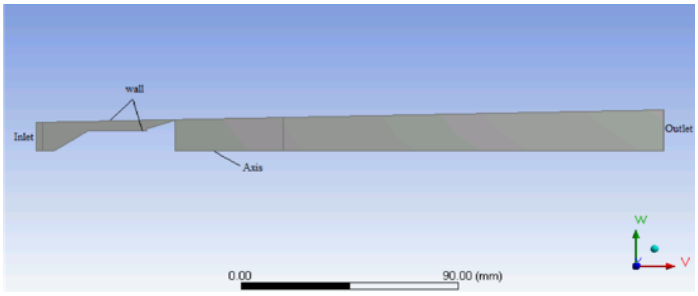

Fig: 3.7 Geometry of 2-D Axisymmetric Model of Rotameter Used for the Analysis

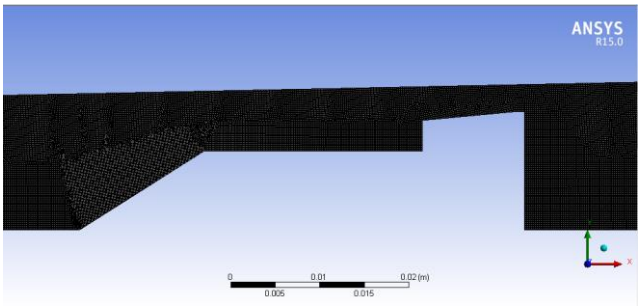

Fig 3.8: Mesh Used around the Float used in the Analysis of Actual Rotameter

The flow domain is discretised using axisymmetric quadrilateral elements. It has been shown that turbulence model SST- k-w model is most suited for the analysis. And hence it is used. Fig.3.7. shows the meshing pattern used for the flow domain. On the surface of the float and the tube face sizing is used. The mesh is around the float as shown in Fig.3.8. The total number of elements is in the range 1.8×10^5 to 2.5×10^5 for the various positions of the float.

The velocity boundary conditions is defined at the inlet corresponding to different float positions of the float. The convergence criteria of 10^{-6} and second order upwind scheme are adopted. The drag force obtained from these conditions are computed at each flow rate and different float positions. The drag force ideally has to be equal to 0.8456 N as per the calculations. The average velocity in the annulus region between the float and tube at each flow rates are the calculated from CFD. The results are tabulated in Table.3.7. The following parameters are given in the Table.3.7.

Q_{ind} is the corresponding flow rate to the assumed position of the float, lpm

Q_{CFD} is the computed flow rate that gives equilibrium of the float at that position lpm

Re is the Reynolds number based on inlet velocity and diameter of the float

$$Re = \frac{\rho . U_{ind} . D_F}{\mu}.$$

U_{CFD} is the inlet velocity from the CFD.

U_{anu} is the average velocity in the annulus region between the float and tapered tube at the position, m/s

F_D is the drag force results obtained from CFD, N

$$C_{D2} = \frac{F_D}{0.5\times\rho\times(U_{anu})^2\times A_F}$$

C_{D2} is the drag coefficient by using U_{anu} as the velocity reference.

Q_{ind} (lpm)	U_{in} (m/s)	Re	U_{CFD}, (m/s)	F_D (N)	QCFD (lpm)	U_{anu} (m/s)	CD_2
4	0.12973	3492	0.12992	0.8453	4.0059	1.44	1.424
7	0.227	6111	0.2282	0.8454	7.0363	1.531	1.26
10	0.325	8749	0.3297	0.8454	10.1659	1.635	1.105
15	0.486	13083	0.4891	0.8455	15.0809	1.694	1.029
20	0.649	17471	0.651347	0.8458	20.0836	1.75	0.96
25	0.8107	21823	0.80875	0.8453	24.9370	1.803	0.908
30	0.9749	26244	0.9708	0.8458	29.9336	1.84	0.873
35	1.135	30553	1.13435	0.8455	34.9765	1.870	0.844
40	1.2973	34922	1.29072	0.8457	39.7981	1.92	0.801

Table 3.7 Results of Flow Rate and Drag Coefficient obtained Using CFD

Results and discussion

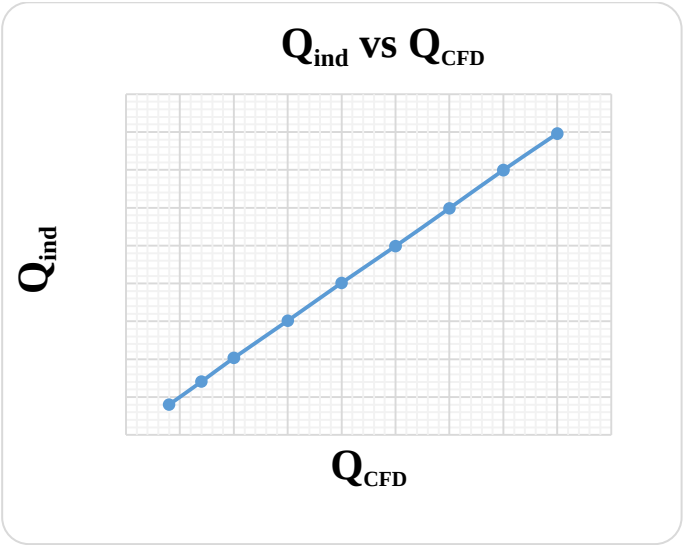

Fig: 3.9 Comparison between Q_{ind} v/s Q_{CFD}

It is observed from the tabulated values of Table 3.7 that the values of Q_{CFD} and Q_{ind} are in very good agreement. Further the values of C_{D2} decrease as the diameter ratio decreases. Fig.3.9 shows comparison between the Q_{in} v/s Q_{CFD}. It can be seen that the values of indicated flow rate and those obtained from CFD are in close agreement.

Fig: 3.10 shows the variation of drag coefficient with Diameter ratio and it is observed that its value increases with incrassating diameter ratio (it can also be observed from Table 3.7).

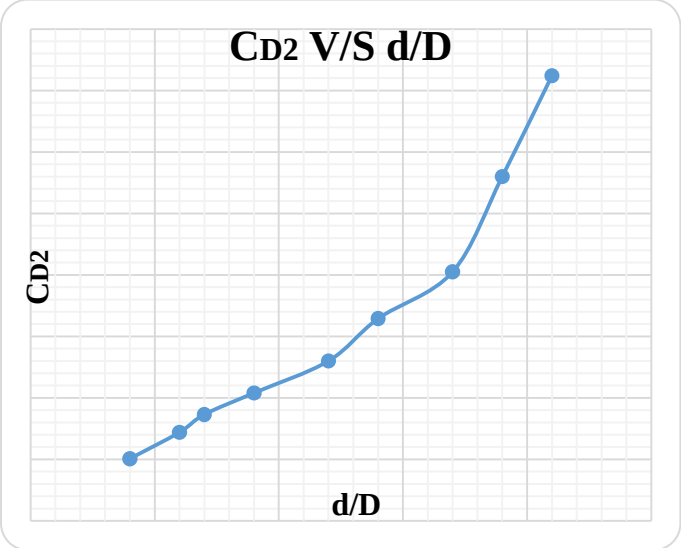

Fig: 3.10 Plot of Drag Coefficient v/s Diameter Ratio

The typical plots of pressure and velocity contours as well as velocity vector plots are shown in Figs. (3.11), (3.12), (3.13).

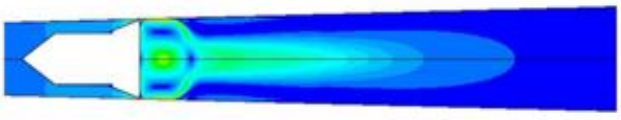

3.11 (a) Velocity Contours for 4 lpm

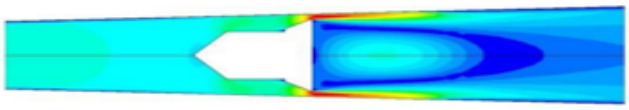

3.11 (b) Velocity Contours for 20 lpm

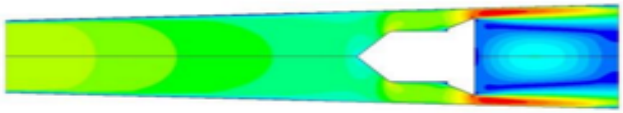

3.11 (c) Velocity Contours for 40 lpm

Fig: 3.11 Different flow rates of velocity contours

3.12 (a) Pressure Contours for 4 lpm

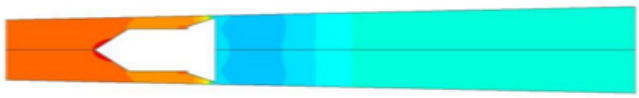

3.12 (b) Pressure Contours for 10 lpm

3.12 (c) Pressure Contours for 30 lpm

Fig: 3.12 Different flow rates of pressure contours

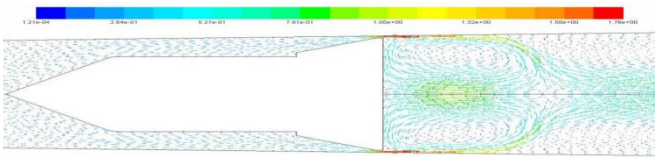

3.13(a) Velocity Vector for 4 lpm

Fig. 3.13 Flow Rate of Velocity Vector

The forgoing analyses has validated the CFD methodology for the analysis of flow through rotameter. Hence this methodology is used in the subsequent analysis reported in this study.

IV. EFFECT ANGLE OF DIVERGENCE ON THE FLOW RANGE OF ROTAMETER

The input data for the design and selection of rotameter for any particular application will consist of properties of the fluid (like viscosity, density rheology,) range of flow rate and size of the pipe.

The rotameter has to be designed by properly choosing the float (material and size), the angle of divergence of the tube, inlet diameter, height etc. The most important parameter that governors the range of flow (for a given inlet diameter and height) is the angle of divergence of tapered tube. Larger this angle wider will be the flow rate ranges. In order to quantify the dependence of flow rate range on $\boldsymbol{\theta}$, the rotameter designed by Deepu et.al [4] is chosen for the investigation.

4.1 Dimensions of the Rotameter Used in Analysis

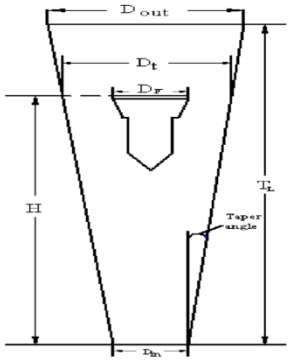

Fig 4.1 Geometrical Specification

Where
Inlet diameter of tapered tube=D_{in}=40mm
Half divergence angle of tapered tube=θ=1.5°
Vertical height of the tube=T_L=300mm
Maximum diameter of the float=D_f=40mm
Height of the float is assumed as=h=50mm
Volume of the float = $V_f = \frac{\Pi}{4} D_f^2 .h$=62831.85mm^3

Deepu et.al [4] have designed a rotameter for measuring rate of water flow in the range 0-100 lpm. In a pipe of 40mm diameter the various dimensions and properties of the float are given in Table 4.1.

Q (lpm)	For Θ=1.5 ° H(mm)
9.99	28.64
20.11	57.29
42.53	112.68
67.41	164.24
94.10	213.90
118.12	259.74

Table 4.1 Actual Values for Different Flow Rates

Deepu et.al [4] has used an angle of divergence $\boldsymbol{\theta}$=1.5°. In the present study this divergence angle is changed and computations have been made for 4 values of $\boldsymbol{\theta}$ is namely 0.25°, 0.5°, 1°, 2° keeping other dimensions as same. Computations have been made for each $\boldsymbol{\theta}$ for different positions of float as given in above Table 4.1.

4.2 Flow Domain, Geometry and Boundary Conditions of the Actual Rotameter for the CFD Analysis

Fig.4.2 shows the geometry of the rotameter inlet diameter 40mm length of the tube is 300mm. 2D axisymmetric model and half of the geometry is shown.

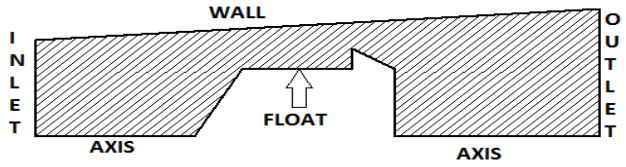

Fig 4.2 Geometry of the Rotameter

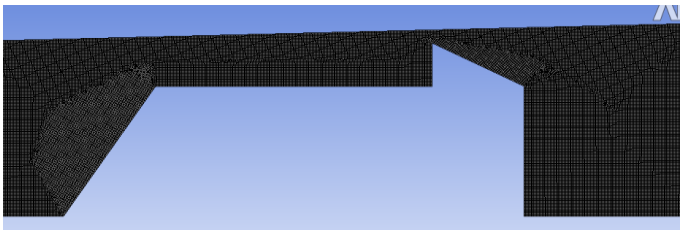

Fig 4.3 Fine Mesh around the Float Using Quadrilateral Elements

Figs.4.2 and 4.3. Shows Geometry and meshing of the flow domain. Here 2D axisymmetric model is considered and hence half of the geometry is shown. The number of elements is in the range 65000 to 90000 with fine mesh elements around float. Axisymmetric quadrilateral elements are used for the discretization. At the inlet velocity defined and gauge pressure is defined zero at the exit. The results from the computation are tabulated in Tables 4.2 to 4.6.In all the computation the fluid to be assumed to be water with density of 1000kg/m^3 and viscosity of 10^{-3} Pas.
At any given $\boldsymbol{\theta}$ and float position the value of C_D is calculated using the value of diameter ratio at that position. For this purpose, the following correlation is proposed by Deepu et.al [4]

$$C_D = 0.4 + \frac{0.882}{\left(1-\frac{d}{D}\right)^{0.3}}$$

The calculated of C_D and the equilibrium drag force are used to calculate the value of velocity in the annulus (U_{ann})

$$F_D = W - F_B = 4.253 = C_{D2} . \frac{1}{2} . \rho . U_{ann}^2 . A_F$$

Then the values of inlet velocity and Q_{cal} are calculated and they are specified as the boundary condition. The computed values of drag force are tabulated and they may not be exactly equal to desired value (4.253 N). In such a case, the actual flow rate (Q_{act}) is calculated using the relationship.

$$Q_{act} = Q_{cal} . \sqrt{\frac{4.253}{(FD)_{CFD}}}$$

The above relation assumes that over a narrow range drag force is proportional to square of the velocity. Finally the actual value of C_D is also tabulated.

H (mm)	D_T (mm)	$\frac{d}{D}$	C_D	U_{anu} (m/s)	Q_{cal} (lpm)	V_{in} (m/s)	$(F_D)_{CFD}$ N	Q_{act} (lpm)	$(C_D)_{CFD}$
28.64	40.25	0.993	4.30	1.254	1.185	0.0157	4.213	1.19	4.26
57.29	40.50	0.987	3.64	1.364	2.586	0.0343	4.202	2.60	3.69
112.68	40.95	0.976	3.10	1.478	5.526	0.0733	4.223	5.54	3.07
164.24	41.43	0.965	2.81	1.552	8.515	0.1129	4.218	8.55	2.78
213.90	41.86	0.956	2.65	1.598	11.457	0.1520	4.216	11.5	2.62
259.74	42.26	0.946	2.51	1.642	14.383	0.1908	4.220	14.4	2.49

Table 4.2 Computed Results for θ=0.25°

Table.4.2. Shows the results of the computation made for half divergence angle θ=0.25°. It is observed that the range of flow rate is approximately 1-15 lpm which is much narrower than that for θ=1.5° which is 10-100 lpm (see Table.4.5). It is also observed that the calculated values of C_D at any given diameter ratio agree very well with the values calculated on the basis of correlation by Deepu et al [4]

$$C_D = 0.4 + \frac{0.882}{\left(1-\frac{d}{D}\right)^{0.3}}$$

H (mm)	D_T (mm)	$\frac{d}{D}$	C_D	U_{anu} (m/s)	Q_{cal} (lpm)	V_{in} (m/s)	$(F_D)_{CFD}$ (N)	Q_{act} (lpm)	$(C_D)_{CFD}$
28.64	40.50	0.987	3.64	1.364	2.586	0.0343	4.202	2.601	3.61
57.29	41.00	0.975	3.06	1.487	5.675	0.0752	4.223	5.695	3.04
112.68	41.95	0.953	2.60	1.613	12.145	0.1610	4.215	12.199	2.57
164.24	42.86	0.933	2.38	1.686	18.825	0.2496	4.232	18.871	2.37
213.90	43.73	0.914	2.24	1.738	25.548	0.3388	4.238	25.593	2.23
259.74	44.53	0.898	2.15	1.774	31.932	0.4235	4.227	32.030	2.13

Table 4.3 Computed Results for θ=0.5°

Table 4.3 shows the results of the computation for the half divergence angle θ=0.5°. It is observed that the range of flow rate is approximately 2.5- 32 lpm

H (mm)	D_T (mm)	$\frac{d}{D}$	C_D	U_{anu} (m/s)	Q_{cal} (lpm)	V_{in} (m/s)	$(F_D)_{CFD}$ (N)	Q_{act} (lpm)	$(C_D)_{CFD}$
28.64	41.00	0.975	3.06	1.487	5.675	0.0753	4.223	5.695	3.04
57.29	42.00	0.952	2.59	1.617	12.496	0.1657	4.215	12.552	2.56
112.68	43.92	0.910	2.21	1.750	27.121	0.3597	4.241	27.159	2.20
164.24	45.73	0.874	2.04	1.822	42.175	0.5593	4.245	42.214	2.03
213.90	47.47	0.842	1.93	1.873	57.662	0.7647	4.237	57.770	1.92
259.74	49.06	0.815	1.86	1.908	72.540	0.9620	4.240	72.651	1.85

Table 4.4 Computed Results for θ=1°

Table 4.4 shows the results of the computation for the half divergence angle θ=1°. It is observed that the range of flow rate is approximately 5-73 lpm.

H (mm)	D_T (mm)	$\frac{d}{D}$	C_D	U_{anu} (m/s)	Q_{cal} (lpm)	V_{in} (m/s)	$(F_D)_{CFD}$ N	Q_{act} (lpm)	$(C_D)_{CFD}$
28.64	41.50	0.963	2.77	1.563	9.00	0.1194	4.218	9.05	2.74
57.29	43.00	0.919	2.27	1.727	20.25	0.2687	4.235	20.29	2.25
112.68	45.90	0.871	2.03	1.826	43.60	0.5785	4.245	43.65	2.02
164.24	48.60	0.823	1.88	1.896	68.07	0.9032	4.239	68.18	1.87
213.90	51.60	0.781	1.79	1.944	97.33	1.2915	4.225	97.65	1.78
259.74	53.60	0.746	1.73	1.978	118.64	1.5740	4.192	119.50	1.70

Table 4.5 Computed Results for θ=1.5°

Table 4.5 shows the results of the computation for the half divergence angle θ=1.5°. It is observed that the range of flow rate is approximately 9- 120 lpm.

Table 4.6 shows the results of the computation for the half divergence angle θ=2°. It is observed that the range of flow rate is approximately 12- 172 lpm.

H (mm)	D_T (mm)	$\frac{d}{D}$	C_D	U_{anu} (m/s)	Q_{cal} (lpm)	V_{in} (m/s)	$(F_D)_{CFD}$ N	Q_{act} (lpm)	$(C_D)_{CFD}$
28.64	42.00	0.952	2.59	1.617	12.496	0.1658	4.213	12.555	2.56
57.29	44.00	0.909	2.21	1.750	27.699	0.3675	4.239	27.774	2.20
112.68	47.83	0.836	1.91	1.883	61.020	0.8097	4.246	61.070	1.90
164.24	51.47	0.777	1.78	1.950	96.408	1.2790	4.218	96.807	1.76
213.90	54.93	0.728	1.70	1.995	133.22	1.7670	4.167	134.63	1.66
259.74	58.13	0.688	1.65	2.025	169.73	2.2520	4.142	171.99	1.60

Table 4.6 Computed Results for θ=2°

4.3 Results and Discussion

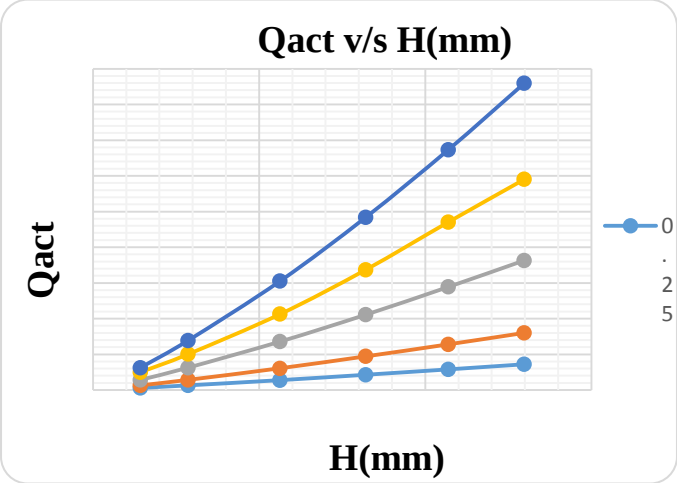

Fig.4.4. Variation of Flow Rate with Float Position for Various Semi Angles of Divergence

Fig.4.4 shows the variation of flow rate with height of the float for various values of ***θ***. It is seen that at any given height the flow rate increases with increasing ***θ***. The dependence is non-linear.

The dependence of maximum flow rate Q_{max} on ***θ*** for this rotameter is shown in Fig.4.5. It is observed that as ***θ*** increases Q_{max} increases none linearly.

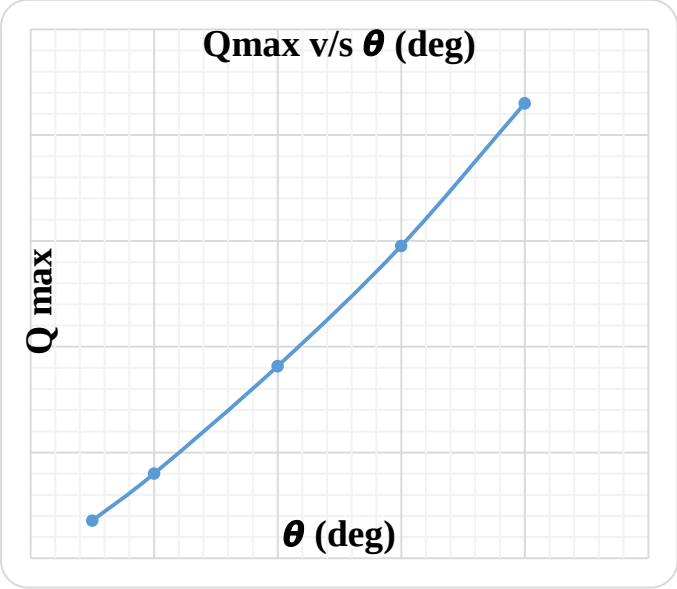

Fig.4.5 Maximum Flow Rate on Angle of Divergence for this Rotameter

Typical pressure and velocity contours as well as velocity vector plots are given in Figs. (4.7), (4.8), (4.9). These plots are drawn for θ=1.5° and flow rate Q= 43.65 lpm. It is observed the pressure drops suddenly as the flow passes over the float, the velocity is maximum in the annulus area between float and tube. The velocity vector plot clearly shows the separated region and re circulating flow behind the float.

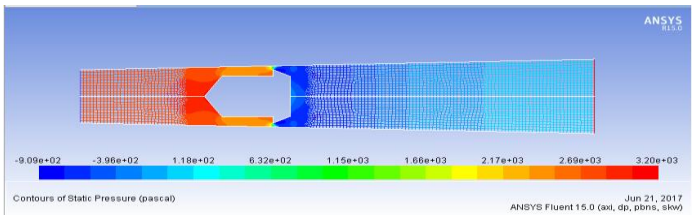

Fig.4.7. Pressure Contours for θ=1.5° and Flow Rate 43.65 lpm

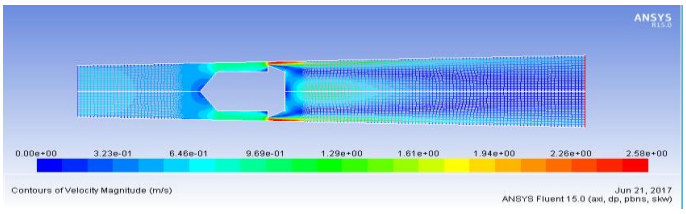

Fig.4.8. Velocity Contours for θ=1.5 and Flow Rate 43.65 lpm

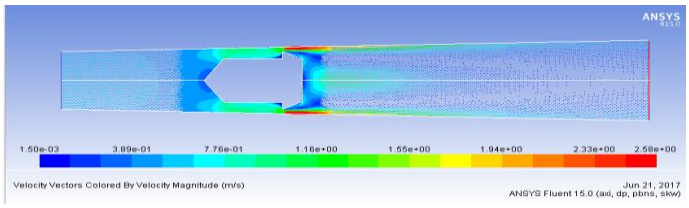

Fig.4.9. Velocity Vector for θ=1.5 and Flow Rate 43.65 lpm

V. DRAG COEFFICIENT OF VISCOSITY COMPENSATING FLOAT IN NON-NEWTONIAN FLUID

Rotameter can be used to measure flow rates both liquid and gases. In most of the applications liquid is Newtonian character. However in many chemical, polymer, as well as petroleum industries it becomes necessary to measure the flow rate of Non-Newtonian fluids. Some examples of non-Newtonian fluids are polymer solutions (like CMC, Polyox,) gums, resins, enamel paints etc.

There are several types of Non-Newtonian fluids like Bingham plastic, power law fluid, yield pseudo plastic etc. A Non-Newtonian fluid is defined as fluid which does not follow Newton's law of viscosity. The relationship between shear stress (ζ) shear rate ( ) is in a Newtonian fluid is given by

$$\zeta=\mu.$$

Where

μ=coefficient dynamic viscosity of the fluid

For a Newtonian fluid μ is a property of liquid which will depend on pressure and temperature. However in a Non-Newtonian fluid shear stress is no longer linearly

proportional to shear rate and hence viscosity becomes dependent on shear rate. One of the most common Non-Newtonian fluid is pseudo plastic fluid or power law fluid. For this fluid the relationship between shear stress and shear rate is given by

$$\tau = K.\dot{\gamma}^{n}$$

Where

n- Power law index

K- Consistency index

The apparent viscosity of the fluid is defined as

$$\mu_{app} = \frac{\tau}{\dot{\gamma}} = \frac{K.\dot{\gamma}n}{\dot{\gamma}} = K.\dot{\gamma}^{(n-1)}$$

For a Newtonian fluid n=1 and hence μ_{app} =k=μ. Hence μ_{app} will be a constant, however for a power law fluid μ_{app} depends on shear rate.

If n<1 μ_{app} decreases with increasing shear rate and hence is called shear thinning fluid and n>1 μ_{app} increases with increasing shear rate and these are called as shear thinking fluid. In petrochemical industries shear thinning fluid are more common (n<1). Hence analysis made for such fluid.

When a rotameter calibrated in water is used to measure pseudo plastic (shear thinning) fluids the indicated flow may not be actual flow rate. Hence it is necessary to study flow of Non-Newtonian fluid through rotameter and understand its effect on the drag force of the float.

5.1 Study on Viscosity Compensating Float

Hence in this chapter drag coefficient of a viscosity compensating float of a rotameter place inside the tube for the flow of Non-Newtonian fluid is investigated. Here viscosity compensating float is taken to be 2D analyses used in ANSYS workbench and geometry is considered as 2D symmetric model. The purpose of analyses for two different diameter ratios namely 0.75, 0.9 and two different Reynolds numbers namely 100 and 500.

Fig.5.1 shows the geometry of the flow domain for viscosity compensating float and diameter ratio is 0.9 as fixed. Upstream length (L_U) is assumed as five times of the inlet diameter of the tube (5D) and downstream length (L_D) is ten times of the inlet diameter of the tube (10D).

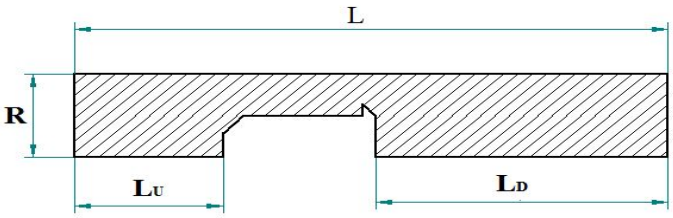

Fig.5.1 Geometry of Viscosity Compensating Float

L- Length of the pipe=330 mm

L_U- Upstream length = 100 mm

L_D-Downstream length = 200mm

R-Radius of the pipe= 10mm

r= maximum radius of float =9 mm

Float Dimensions In mm

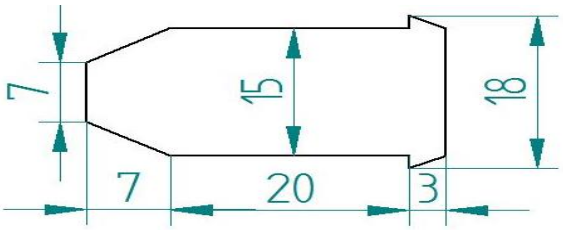

Fig.5.2 Float Dimensions of Rotameter.

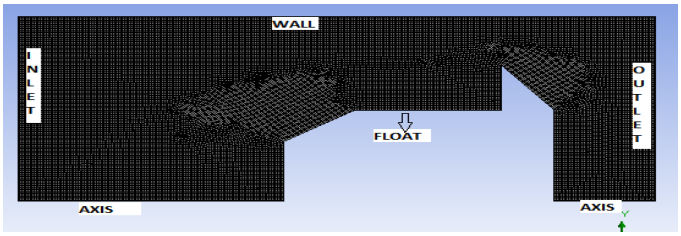

Fig.5.3 Meshing and Boundary condition of Viscosity Compensating Float

Fig.5.3. shows that meshing of geometry and boundary condition of the flow domain. In the boundary condition at the input data is velocity 1m/s, density 1000kg/m^3, and outlet gauge pressure is zero. Here meshing is done by using quadrilateral elements and fine refinement at the wall and float. Chosen convergence criteria 10^{-6} is given. And approximately 75000 elements are used in this analyses.

The fluid is assumed to incompressible and follow power law model. Hence $\tau = K.\dot{\gamma}^{n}$ the values of k and n are specified as input data for power law fluid. The definition of Reynolds number is modified is given as

$$Re_{PL} = \frac{\rho U^{2-n} D^{n}}{k\left[\frac{3n+1}{4n}\right]^{n} 8^{n-1}}$$

It is observed for a Newtonian fluid (n=1) Re_{PL}=Re (k=μ). Analyses have been made for different values of n namely n=1, 0.8, 0.6, 0.4, 0.2. For each of the power law index the value of k is computed so that Reynolds number for all fluids will have the same value.

5.2 Range of Parameters Studied

The values of density (ρ), velocity (V), diameter (D), are taken as constant. Hence ρ= 1000kg/m^3, V=1m/s, D=20mm. Computations have been made for two diameter ratios namely d/D=0.9, 0.75. CFD analyses have been used to compute drag force on the float. The coefficient drag is calculated from this data. Analysis have been made at these to Reynolds number for 5 power law fluids having n=1, 0.8, 0.6, 0.4, 0.2.

As mentioned before computation have been made for two Reynolds numbers namely 100 and 500. Tables.5.1 and 5.2. Given the computed values of F_D and C_D for different values of n. It is to be noted the value of k for each case is chosen so that power law Reynolds number remains same any set of data. It is observed from this table that any given Reynolds numbers F_D decreases as the value of n also decreases similarly trend is also observed in C_D. Further at any given value of n the value of C_D decreases with increasing Reynolds number. The range of Reynolds number chosen in this analyses are in the laminar regime. Since the effect of non-Newtonian behaviour is more predominant in laminar regime the data presented in these Tables corresponds to diameter ratio of 0.9.

n	k	F_D	C_D
1	0.20	17.18	109.4
0.8	0.63	12.32	78.44
0.6	2.00	10.34	65.83
0.4	6.42	9.65	61.44
0.2	21.00	9.45	60.10

Table. 5.1 Computed Values of drag coefficient in the flow of non - Newtonian fluid for Re=100 (ρ=1000kg/m^3, v=1m/s, D=0.05m, d/D=0.9

n	k	F_D	C_D
1	0.04	8.617	54.86
0.8	0.1263	8.039	51.18
0.6	0.4006	7.876	50.15
0.4	1.282	7.755	49.37
0.2	4.202	7.724	49.18

Table. 5.2 Computed Values of drag coefficient in the flow of non - Newtonian fluid for Re=500 (ρ=1000 kg/m^3, v=1m/s, D=0.05m, d/D=0.9

Tables.5.3 and 5.4. Give the results for diameter ratio 0.75. It is observed that the trends of F_D and C_D with a variation n in similar. However the values of F_D and C_D at this diameter ratio are much smaller as compared to d/D = 0.9.

n	k	F_D	C_D
1	0.20	4.268	27.17
0.8	0.63	3.608	22.97
0.6	2.00	3.135	19.96
0.4	6.42	2.801	17.83
0.2	21.00	2.598	15.28

Table. 5.3 Computed Values of drag coefficient in the flow of non - Newtonian fluid for Re=100 (ρ=1000kg/m^3, v=1m/s, D=0.05m, d/D=0.75

n	k	F_D	C_D
1	0.20	1.486	9.46
0.8	0.63	1.329	8.47
0.6	2.00	1.222	7.78
0.4	6.42	1.170	7.45
0.2	21.00	1.142	7.27

Table. 5.4 Computed Values of drag coefficient in the flow of non - Newtonian fluid for Re=500(ρ=1000kg/m^3, v=1m/s, D=0.05m, d/D=0.75

5.3 Results and Discussions

Figs. 5.4 and 5.5 so the variation of C_D with respect to n for 2 diameter ratios namely 0.9 and 0.75 respectively. This Figs graphically confirm the variation of C_D with n as described earlier. Since value of C_D depends on n it can be expect that the float position in rotameter will change with change in the value of n.

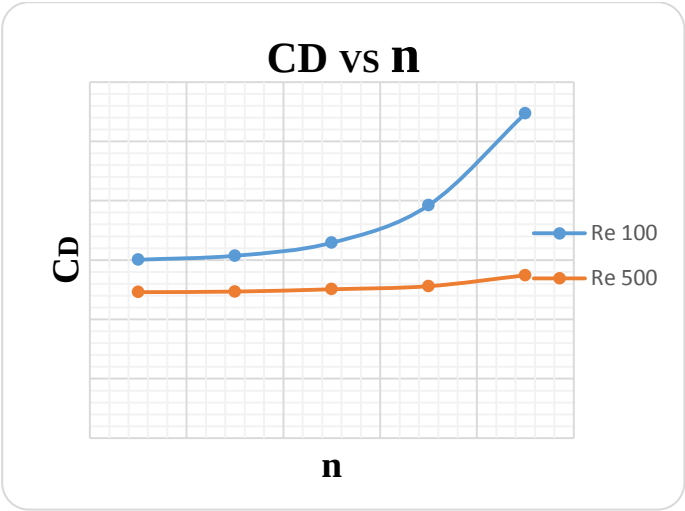

Fig.5.4 Variation of C_D for Power Law Index with Diameter Ratio 0.9

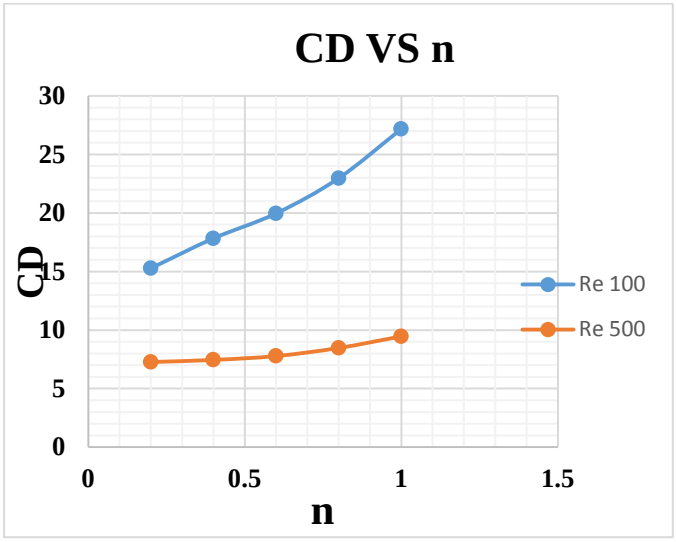

Fig. 5.5 Variation of C_D for Power Law Index with Diameter Ratio 0.75

Typically plots are pressure and velocity contours as well as velocity plot are given in Figs.5.6, 5.7, 5.8. These plots are drawn for diameter ratio 0.9 and Reynolds number 500.

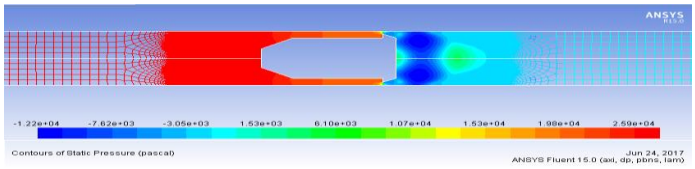

Fig.5.6 Pressure Contours

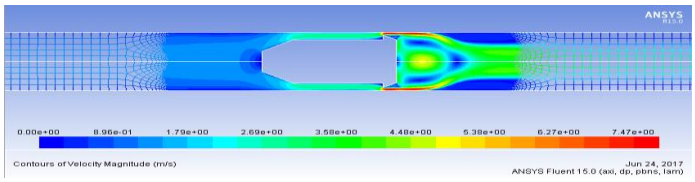

Fig.5.7 Velocity Contours

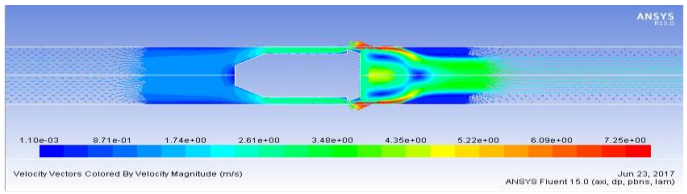

Fig. 5.8 Velocity Vector

VI. METERING OF NON-NEWTONIAN FLUIDS BY ROTAMETER

The computations discussed in the previous chapter have shown that the drag force on the float in a rotameter is affected by the non- Newtonian of fluid. Hence when a rotameter calibrated in water is used to measure flow rate of power law fluids the indicated flow rate may not be exactly equal to actual flow rate. In order to study this effect, the flow of power law fluid through on actual rotameter is analysed and the results are presented this chapter.

6.1 Details of Rotameter Used in Analysis

The rotameter which is used for this analysis is the one which exits in fluid mechanics laboratory. The various dimensions and specifications of this rotameter have already been given in section (3.3) of chapter 3 under the validation and methodology. The various dimension and specification are given briefly Figs.6.1and 6.2. For the sake of completeness.

A) Dimensions of the Tapered Tube:

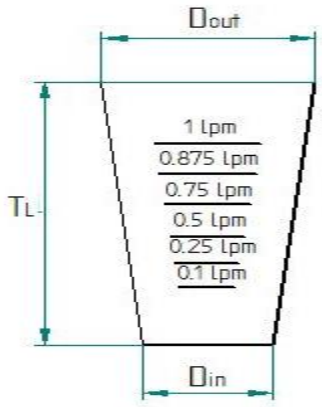

Fig. 6.1 Dimensions of the Tapered tube

Where

Inlet diameter = D_{in} = 25.48mm

Outlet diameter = D_{out}=36.85mm

Vertical height of the tube= T_L=260mm

Half Taper angle = θ= 1.12˚.

B) Dimensions of the float:

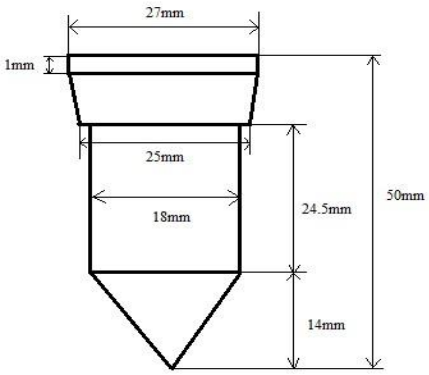

Fig.6.2 Dimensions of the Float

Material Density = ρ_F= 1080 kg/m^3

Water Density = ρ_w= 1000 kg/m^3

Volume of float= V_F = 12584.46 mm^3

It is well known that Non-Newtonian effect is more predominant in laminar flow. Hence the range of flow rate for this rotameter has been modified to 0-1 lpm, so

that the flow is in the laminar regime for water flow. As a first step characteristics of rotameter is analysed for water flow in the range 0.1 to 1 lpm. In order to accommodate this reduction in the flow rate the density of the float is modified to 1080 kg/m^3 while keeping all the dimensions as constant.

Thus equilibrium drag force now becomes

$F_D = (\rho_F - \rho_W) \times V_F \times g$

$= (1080-1000) \times 12584.46 \times 10^{-9} \times 9.81$

$= 9.81 \times 10^{-3}$ N

As a first step the characteristics of rotameter with water flow is established.

C) Flow rate markings

Flow rate markings on the glass tube have been modified at various intervals in the range 0.1-1 lpm. The heights of each marking from the inlet have been measured and the ratio of diameter of the float and diameter of the tapered tube at float position are tabulated in Table.6.1

Q_{ind} (lpm)	H (mm)	$\frac{D_F}{D_t}$
0.1	57.5	0.968
0.25	86.5	0.927
0.5	129	0.874
0.75	166	0.823
0.875	183	0.814
1	199	0.798

Table.6.1 Height of markings from Inlet (Float Height)for different Flow rates and Diameter ratio at that position

6.2 Flow Domain and Boundary Conditions Used In CFD Modelling

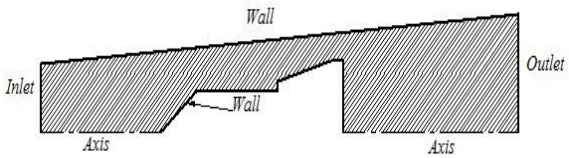

Fig.6.3 Geometry and Boundary Conditions Used for the Analysis of Actual Rotameter

Fig.6.3 shows the geometry of flow domain and boundary conditions used in CFD analysis. Geometry is considered as 2D axisymmetric and hence only half of the domain is analysed. The float is placed at different positions corresponding to different flow rates in the range 0.1-1 lpm. For different flow rates the inlet velocities corresponding to that flow rate is specified as boundary condition at the inlet of the pipe (see Table 6.2).The 2D axisymmetric model is constructed using ANSYS software design modeller.

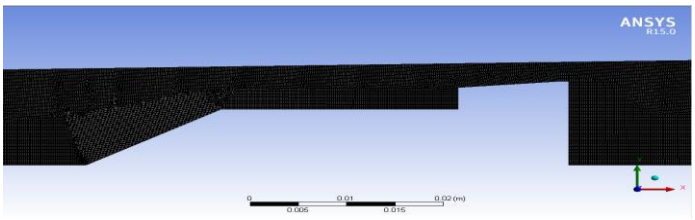

Fig.6.4 Mesh Used around the Float Used in the Analysis of Actual Rotameter

Since the diameter of the tapered tube increases the number of elements also around the float increases uniformly as the float position and flow rate also increases. The options used for meshing is face sizing, refinement and face split (for the fine mesh around the float). And convergence criteria 10^{-6} been set. For equilibrium of the float the drag force has to be equal to $9.81*10^{-3}$ N as per the calculations.

6.3 CFD Analysis of Water Flow through Rotameter

The flow of water through in the rotameter at various positions of the float are analysed and at each position the inlet velocity (hence the flow rate) at which the equilibrium drag force is computed using CFD. The procedure and other details are already given in chapter 3.3 and hence are not repeated here. The results from the computation are given in Table.6.2

Q (lpm)	H (mm)	$\frac{d}{D}$	U_{in} (m/s)	F_D (N)	U_{corr} (m/s)	F_{Dcal} (N)	C_D	R_e w	Q_w (lpm)
0.1	57.5	0.968	0.00326	0.0564	0.00136	0.00979	102.12	84	0.0417
0.25	86.5	0.927	0.00817	0.01984	0.00571	0.00980	34.50	208	0.175
0.5	129	0.874	0.0163	0.00981	0.0163	0.00981	15.38	415	0.500
0.75	166	0.823	0.0245	0.00690	0.0292	0.00979	9.92	624	0.894
0.875	183	0.814	0.0286	0.00615	0.0361	0.00980	8.50	729	1.105
1	199	0.798	0.0326	0.00563	0.0431	0.00978	7.47	840	1.320

Table.6.2. Computed Results for Water Flow

For this analysis water properties are taken as ρ=1000kg/m3, $\mu=10^{-3}$ Pas,

It is observed that the range of Reynolds number is 84 to 840 for the range of flow rate 0.1 to 1 lpm. For the initially specified value of flow velocity, the computed drag will not be equal to equilibrium value. Hence the inlet velocity modified by using standard procedure to obtain the required drag force. The calculated value of the flow rate is given as Q_{cal} in the Table. The flow is in the laminar regime. And the values of Re are also given in Table.6.2. It is also observed that the value of C_D decreases with decreasing diameter ratio and increasing Reynolds number. These trends have been discussed earlier.

6.4 Analysis of the Flow of Power Law Fluid through Rotameter at Equivalent Reynolds Number

CFD analyses have been made for the flow of power law fluid having different values of K and n have been made for this rotameter. For any given value of n and the position of the float the value of K is calculated so that the power law Reynolds number corresponding to the same inlet velocity is equal to the Reynolds number obtained from water flow at that position of the float. Using this value of K as input data the drag force on the float is calculated. In case this is not equal to the equilibrium force, the inlet velocity is modified as per the procedure already discussed. Hence the flow rate of the fluid for various positions of the float (Q_{pl}) are calculated for each value of n. The results are presented in Tables.6.3.

For this analysis, properties of the fluid are ρ=1000kg/m^3.the values of k and n are specified.

H (mm)	R_{ew}	k	U_{in} (m/s)	F_{Dcal} (N)	U_{corr} (m/s)	C_D	Q_w (lpm)	Q_{PL} (lpm)	% Error
57.5	84	9.78×10^{-4}	0.00136	0.00978	0.00139	98.12	0.0417	0.0425	-1.92
86.5	208	1.07×10^{-3}	0.00571	0.00979	0.00574	33.86	0.1750	0.1769	-1.08
129	415	1.14×10^{-3}	0.0163	0.00980	0.0165	15.22	0.500	0.5040	-0.80
166	624	1.19×10^{-3}	0.0292	0.00978	0.0296	9.62	0.894	0.9055	-1.29
183	729	1.21×10^{-3}	0.0361	0.00980	0.0365	8.34	1.105	1.118	-1.18
199	840	1.23×10^{-3}	0.0431	0.00979	0.0435	7.38	1.320	1.344	-1.82

Table.6.3 (a) Computed Values of drag coefficient in the flow of non -Newtonian fluid for n=0.9

H (mm)	R_{ew}	k	U_{in} (m/s)	F_{Dcal} (N)	U_{corr} (m/s)	C_D	Q_w (lpm)	Q_{PL} (lpm)	% Error
57.5	84	9.57×10^{-4}	0.00136	0.00976	0.00140	97.50	0.0417	0.0429	-2.87
86.5	208	1.15×10^{-3}	0.00571	0.00977	0.00577	33.75	0.175	0.177	-1.14
129	415	1.32×10^{-3}	0.0163	0.00979	0.0166	15.41	0.500	0.5080	-1.60
166	624	1.43×10^{-3}	0.0292	0.00978	0.0299	10.81	0.894	0.915	-2.35
183	729	1.47×10^{-3}	0.0361	0.00977	0.0368	8.77	1.105	1.126	-1.90
199	840	1.51×10^{-3}	0.0431	0.00977	0.0439	7.55	1.320	1.346	-1.81

Table.6.3 (b) Computed Values of drag coefficient in the flow of non -Newtonian fluid for n = 0.8

H (mm)	R_{ew}	k	U_{in} (m/s)	F_{Dcal} (N)	U_{corr} (m/s)	C_D	Q_w (lpm)	Q_{PL} (lpm)	% Error
57.5	84	9.21×10^{-4}	0.00136	0.00978	0.00141	99.82	0.0417	0.0431	-3.35
86.5	208	1.32×10^{-3}	0.00571	0.00976	0.00580	33.93	0.175	0.1774	-1.37
129	415	1.75×10^{-3}	0.0163	0.00981	0.0168	15.31	0.500	0.514	-2.80
166	624	2.06×10^{-3}	0.0292	0.00978	0.0302	9.84	0.894	0.924	-3.36
183	729	2.19×10^{-3}	0.0361	0.00977	0.0369	8.43	1.105	1.129	-2.17
199	840	2.31×10^{-3}	0.0431	0.00978	0.0441	7.36	1.320	1.349	-2.19

Table.6.3 (c) Computed Values of drag coefficient in the flow of non -Newtonian fluid for n=0.6

H (mm)	R_{ew}	k	U_{in} (m/s)	F_{Dcal} (N)	U_{corr} (m/s)	C_D	Q_w (lpm)	Q_{PL} (lpm)	% Error
57.5	84	8.94×10^{-4}	0.00136	0.00979	0.00142	99.92	0.0417	0.0434	-4.07
86.5	208	1.55×10^{-3}	0.00571	0.00980	0.00581	33.64	0.175	0.178	-1.71
129	415	2.34×10^{-3}	0.0163	0.00981	0.0169	15.31	0.500	0.517	-3.40
166	624	2.68×10^{-3}	0.0292	0.00979	0.0304	9.59	0.894	0.930	-4.02
183	729	3.28×10^{-3}	0.0361	0.00980	0.0372	8.41	1.105	1.138	-2.98
199	840	3.55×10^{-3}	0.0431	0.00978	0.0443	7.34	1.320	1.355	-2.65

Table.6.3 (d) Computed Values of drag coefficient in the flow of non -Newtonian fluid for n=0.4

H (mm)	R_{ew}	k	U_{in} (m/s)	F_{Dcal} (N)	U_{corr} (m/s)	C_D	Q_w (lpm)	Q_{PL} (lpm)	% Error
57.5	84	8.77×10^{-4}	0.00136	0.00977	0.00143	99.72	0.0417	0.0437	-4.79
86.5	208	1.85×10^{-3}	0.00571	0.00980	0.00583	33.43	0.175	0.178	-1.73
129	415	3.22×10^{-3}	0.0163	0.00981	0.0170	15.25	0.500	0.520	-4.03

166	624	4.45×10^{-3}	0.0292	0.00980	0.0305	9.57	0.894	0.933	-4.36
183	729	5.03×10^{-3}	0.0361	0.00978	0.0375	8.36	1.105	1.147	-3.80
199	840	5.53×10^{-3}	0.0431	0.00977	0.0445	7.27	1.320	1.361	-3.10

Table.6.3 (e) Computed Values of drag coefficient in the flow of non -Newtonian fluid for n=0.2

Table.6.3 Rotameter Performance with Pseudo Plastic Fluid for Various Values of n and k Value Adjusted to give equal Reynolds Number in water

Tables 6.3. gives the computed values for various values of n. It is to be noted that the value of k for each flow rate is calculated so that the power law Reynolds number becomes equal to Reynolds number for water at that position. Hence in this analyses we are comparing the performance of rotameter with pseudo plastic fluid when Reynolds numbers are same in the both water flow and liquid flow. For any given float position inlet velocity is specified as the same value that exits for water. However the data will not be corresponding to any single fluid since the value of k changes with flow rate. The computed values of k for each individual n are given in the Tables. As an initial guess the inlet velocity corresponding to water flow is given and drag force on float is computed. Then this velocity is corrected to in order to obtain designed drag force. The flow rates at which this occurs are also tabulated as $Q_{PL.}$ The deviations between Q_{PL} and Q_W are calculated and are given in the Table.6.3.

Hence if the rotameter is calibrated in water and is used for measuring the flow of power law fluid Q_{PL} is the actual flow rate whereas Q_W will be the flow indicated by the meter. The difference between these two represents error in the measurement. It is observed that the tabulated values that Q_{PL} are always larger than Q_W and the % Error depends on the value of n. However the errors are not very large.

The average % Errors are - (1.340), (1.945), (2.54), (3.138), (3.63) for n=0.9, 0.8, 0.6, 0.4, 0.2 respectively.
It is observed as the value of n decreases errors are increasing. This conclusion is valid only when Reynolds number during measurement is same as that for water flow.

6.5 Analysis of Flow through Rotameter of Non-Newtonian Fluid (With Constant k)

In the previous section, the value of k for any given value of n was changing with position of float in order to keep Reynolds number same both in water as well as non- Newtonian fluid. In the present analysis, for a particular value of n the value of k is calculated for the float position corresponding to H= 129mm, at this flow rate in order to achieve the same values Re. Thus at this position both Re_{PL} and Rew are equal. This value of k is kept constant for at other flow rates for any given value of n. Hence this analysis corresponds to metering of a single fluid by the rotameter. The results are tabulated in Tables.6.4. (a) to (e).

It is observed from the tabulated values that at lower flow rates Repl will be less than Rew whereas reverse is true at higher flow rates. This effect becomes more prominent with decreasing value of n. Thus it is observed that from Table.6.4. (e). for H=57.5mm R_{ew}= 84 and R_{epl}=23. However for the same value of n at H=199mm, R_{ew}= 1100, R_{epl}=1443.

H (mm)	U_{in} (m/s)	F_{Dcal} (N)	U_{corr} (m/s)	C_D	R_{ew}	R_{epL}	Q_w (lpm)	Q_{PL} (lpm)	% Error
57.5	0.00136	0.00978	0.00142	98.12	84	71	0.0417	0.0434	-4.07
86.5	0.00571	0.00979	0.00580	33.86	208	196	0.175	0.178	-1.73
129	0.0163	0.00980	0.0165	15.22	415	419	0.500	0.5040	-1.08
166	0.0292	0.00978	0.0299	9.62	624	655	0.894	0.915	-2.34
183	0.0361	0.00980	0.0368	8.34	729	777	1.105	1.125	-1.80
199	0.0431	0.00979	0.0441	7.38	840	897	1.320	1.349	-2.19

Table.6.4 (a) Computed Values of drag coefficient in the flow of non - Newtonian fluid for n=0.9 ($K=1.14\times10^{-3}$)

H (mm)	U_{in} (m/s)	F_{Dcal} (N)	U_{corr} (m/s)	C_D	R_{ew}	R_{epL}	Q_w (lpm)	Q_{PL} (lpm)	% Error
57.5	0.00136	0.00976	0.00145	97.50	84	60	0.0417	0.0441	-5.75
86.5	0.00571	0.00977	0.00586	33.75	208	182	0.175	0.179	-2.28
129	0.0163	0.00979	0.0166	15.41	415	416	0.500	0.5080	-1.60
166	0.0292	0.00978	0.0303	10.81	624	677	0.894	0.926	-3.58
183	0.0361	0.00977	0.0372	8.77	729	816	1.105	1.138	-2.98
199	0.0431	0.00980	0.0444	7.55	840	955	1.320	1.358	-2.87

Table.6.4 (b) Computed Values of drag coefficient in the flow of non - Newtonian fluid for n=0.8 ($K=1.32\times10^{-3}$)

H (mm)	U_{in} (m/s)	F_{Dcal} (N)	U_{corr} (m/s)	C_D	R_{ew}	Re_{pL}	Q_w (lpm)	Q_{PL} (lpm)	% Error
57.5	0.00136	0.00978	0.00149	99.82	84	R_e	0.0417	0.0447	-7.19
86.5	0.00571	0.00976	0.00588	33.93	208	158	0.175	0.178	-1.71
129	0.0163	0.00981	0.0168	15.31	415	416	0.500	0.514	-2.80
166	0.0292	0.00978	0.0305	9.84	624	735	0.894	0.933	-4.36
183	0.0361	0.00977	0.0375	8.43	729	913	1.105	1.147	-3.80
199	0.0431	0.00978	0.0448	7.36	840	1098	1.320	1.370	-3.78

Table.6.4 (c) Computed Values of drag coefficient in the flow of non - Newtonian fluid for n=0.6 ($K=1.175\times10^{-3}$)

H (mm)	U_{in} (m/s)	F_{Dcal} (N)	U_{corr} (m/s)	C_D	R_{ew}	Re_{pL}	Q_w (lpm)	Q_{PL} (lpm)	% Error
57.5	0.00136	0.00979	0.00151	99.92	84	32	0.0417	0.0454	-8.87
86.5	0.00571	0.00980	0.00592	33.64	208	138	0.175	0.181	-3.42
129	0.0163	0.00981	0.0169	15.31	415	415	0.500	0.517	-3.40
166	0.0292	0.00979	0.0308	9.59	624	799	0.894	0.942	-5.36
183	0.0361	0.00980	0.0380	8.41	729	1023	1.105	1.162	-5.15
199	0.0431	0.00978	0.0453	7.34	840	1262	1.320	1.385	-4.92

Table.6.4 (d) Computed Values of drag coefficient in the flow of non - Newtonian fluid for n=0.4 ($K=2.34\times10^{-3}$)

H (mm)	U_{in} (m/s)	F_{Dcal} (N)	U_{corr} (m/s)	C_D	R_{ew}	Re_{pL}	Q_w (lpm)	Q_{PL} (lpm)	% Error
57.5	0.00136	0.00977	0.00155	99.72	84	23	0.0417	0.0461	-10.55
86.5	0.00571	0.00980	0.00594	33.43	208	120	0.175	0.182	-4.00
129	0.0163	0.00981	0.0170	15.25	415	415	0.500	0.520	-4.03
166	0.0292	0.00980	0.0309	9.57	624	863	0.894	0.945	-5.70
183	0.0361	0.00978	0.0384	8.36	729	1141	1.105	1.174	-6.24
199	0.0431	0.00977	0.0457	7.27	840	1443	1.320	1.398	-5.90

Table.6.4 (e) Computed Values of drag coefficient in the flow of non - Newtonian fluid for n=0.2 ($K=3.22\times10^{-3}$)

Table.6.4. Rotameter Performance with Pseudo Plastic Fluid for Various Values of n

It is observed form the tabulated values of the % errors between Q_{pl} and Q_w have increased as compared to the earlier case when the Re are kept same. Again deviation increase with decrease in the value of n

Typical pressure and velocity contours plot as well as velocity vector plot for the flow of non-Newtonian fluid are shown in Figs.6.5, 6.6, 6.7. These plots are drawn for θ=1.12° and flow rate 0.5 lpm and n =0.9

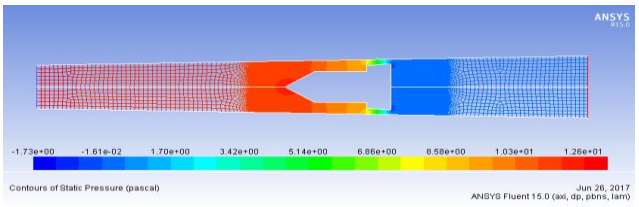

Fig.6.5 Pressure Contours for Q= 0.5 lpm

VII. CONCLUDING REMARKS

7.1 Major conclusions

The various conclusion that have been drawn from different aspects of the present work have already been given in various chapters of thesis. The following general conclusions can be drawn.

- A validated CFD methodology can be used to accurately predict the performance of rotameter. However care has to be taken to properly discretize the domain and choose proper turbulence model.
- The angle of divergence of tapered tube has a marked influence on the range of flow rate that can be measured in a rotameter. Usually this semi angle of divergence is chosen in the range 0.5°to 2°. The effect of θ on the maximum flow rate is quantified for a given rotameter.
- The drag characteristics of a viscosity compensating float inside a pipe for the flow of pseudo plastic fluid have been studied this has been done for two diameter ratios and two Reynolds numbers in the laminar regime. It is observed that the value of C_D is affected by the values of k and n.
- When a rotameter calibrated in water is used to measure the flow of non-Newtonian fluid, the indicated flow will always be less than actual flow as long as Reynolds numbers are in same range. The error in measurement increases with decreasing value of power law index.
- The maximum error will be of order of -5% as long as care is taken to ensure the Re numbers are in the same range as that of water and flow is in the laminar regime.

7.2 Scope for Future Work

This work can be extended to include additional parameters. Some of them are listed below.

- The fluid has been assumed as incompressible for the present analyses. The compressibility effect on flow metering by rotameter can be studied. This will be particularly useful for metering of gases at low pressures.
- The work can be extended to other types of non-Newtonian fluids like Bingham plastic, yield pseudo plastic etc.
- The effect of unsteadiness in the flow as well as upstream disturbances can also be studied for both Newtonian and non-Newtonian fluids.

VIII. REFERENCES

[1]. Arun R, Yogesh kumar K J, Dr. V. Seshadri. "*CFD analysis of the effect of defects in welding and surface finish on the performance characteristics of venturimeter"*. International journal of emerging technology and advanced engineering (IJETAE). ISSN 2250-2459, *Volume-5, issue 6, June 2015,*

[2]. Rakesh Joshi "*The effect of rotameter float design on the performance characteristics of rotameter"*. International Journal of Engineering and Technical Research (IJETR). *ISSN: 2321-0869, Volume-3, Issue-, December 2013,*

[3]. Prasanna M A, Dr. V Seshadri, Yogesh Kumar K J, "*Analysis of compressible effects in the flow metering by orifice plate using CFD*" International journal of scientific research in science engineering and technology (IJSRSET). *ISSN 2395-1990, volume-2, issue 4, 2016.*

[4]. Deepu C N, Yogesh Kumar K J, Dr. V Seshadri, "*Design analysis for a rotameter using CFD*" International journal of engineering science and research technology (IJESRT). ISSN 2277-9655, volume-3, June 2016.

[5]. Pavan Kumar K P, Dr. V Seshadri, Puneeth kumar S B, Analysis of flow through rotameter using CFD" International journal of emerging technology and advanced engineering (IJETAE). ISSN 2250-2459, volume-5 issue-6, June 2015.

[6]. T. Sarpakaya, "Flow on Non-Newtonian Fluids in a Magnetic Field," *AIChE Journal*, Vol. 7, 1961, pp. 26-28.

[7]. I. A. Hassanien, A. A. Abdullah and R. S. R. Gorla, "Flow and Heat Transfer in a Power-Law Fluid over a Non-Isothermal Stretching Sheet," *Mathematical and Computer Modelling*, Vol. 28, No. 9, 1998, pp. 105-116. doi:10.1016/S0895-7177(98)00148-4

[8]. A. Acrivos, M. J. Shah and E. E. Peterson, "Momentum and Heat Transfer in Laminar Boundary Layer Flows of Non-Newtonian Fluids past External Surfaces," *AIChE Journal*, Vol. 6, No. 2, 1960, pp. 312-317. doi:10.1002/aic.690060227